AEDC-TDR-62-104

DESCRIPTION OF TERMINAL BALLISTICS RANGES

By

E. H. Goodman

von Kármán Gas Dynamics Facility
ARO, Inc.

TECHNICAL DOCUMENTARY REPORT NO. AEDC-TDR-62-104

May 1962

AFSC Program Area 750A, Project 8871, Task 88509

(Prepared under Contract No. AF 40(600)-800 S/A 24(61-73) by ARO, Inc., contract operator of AEDC, Arnold Air Force Station, Tennessee.)

ARNOLD ENGINEERING DEVELOPMENT CENTER

AIR FORCE SYSTEMS COMMAND

UNITED STATES AIR FORCE

NOTICES

Qualified requesters may obtain copies of this report from ASTIA. Orders will be expedited if placed through the librarian or other staff member designated to request and receive documents from ASTIA.

When Government drawings, specifications or other data are used for any purpose other than in connection with a definitely related Government procurement operation, the United States Government thereby incurs no responsibility nor any obligation whatsoever; and the fact that the Government may have formulated, furnished, or in any way supplied the said drawings, specifications, or other data, is not to be regarded by implication or otherwise as in any manner licensing the holder or any other person or corporation, or conveying any rights or permission to manufacture, use, or sell any patented invention that may in any way be related thereto.

DESCRIPTION OF TERMINAL BALLISTICS RANGES

By

E. H. Goodman
von Kármán Gas Dynamics Facility
ARO, Inc.
a subsidiary of Sverdrup and Parcel, Inc.

May 1962

ARO Project No. 386144

AF - AEDC
Arnold AFS Tenn

ABSTRACT

The AEDC Terminal Ballistics Ranges and available instrumentation systems are described. Current launcher performance, instrumentation, and data reduction technique are presented.

CONTENTS

	Page
ABSTRACT	ii
1.0 INTRODUCTION	1
2.0 LAUNCHER SYSTEMS FOR RANGES	1
3.0 RANGES	2
4.0 INSTRUMENTATION FOR RANGES	3
5.0 PHYSICS OF CRATER FORMATION	
5.1 Stress Analysis of Craters	4
5.2 Radiation Measurements	4
APPENDIX I - Data Reduction	15

TABLE

1.	Description of Terminal Ballistics Ranges	5

ILLUSTRATIONS

Figure		
1.	S-2 Terminal Ballistics Range	6
2.	S-1 and S-2 Terminal Ballistics Ranges	7
3.	Performance of S-1 and S-2	8
4.	Instrumentation for S-1 and S-2	9
5.	Observation of Hypervelocity Impact Phenomena	
	a. 17,600 fps	10
	b. 21,800 fps	11
6.	Dimensions of Aluminum Impact Craters in Semi-Infinite Aluminum Targets	
	a. Volume	12
	b. Diameter	13
	c. Depth	14

1.0 INTRODUCTION

During the latter part of fiscal year 1961, the von Kármán Gas Dynamics Facility (VKF) of the Arnold Engineering Development Center (AEDC), Air Force Systems Command (AFSC), USAF, was given the responsibility of developing and operating two Terminal Ballistics Ranges. (These ranges will be referred to as Range S-1 and Range S-2 in this report.) A third range (S-3) is now nearing completion.

Figure 1 shows the general layout of Range S-2 which is representative in configuration of the Terminal Ballistics Ranges. Basically, it is as follows:

1. A two-stage launcher system which is coupled to
2. An expansion chamber -- The purpose of the expansion chamber is to allow the propellant gas to diffuse and not proceed downrange in front of the projectile. Also, the expansion chamber prevents the diverging part of the sabot from proceeding downrange. This occurs when the sabot is stripped from the projectile as it leaves the launch tube muzzle.
3. The connecting tube between the expansion tanks and the target tank -- This tube provides longitudinal placement and port housings for the
4. Shadowgraph stations -- The three shadowgraph stations are set 5 ft apart, and one is set orthogonally to the other two.
5. The target chamber houses the target material, has viewing ports for the high-speed framing camera, and furnishes a mount and housing for the preimpact events such as prestressing or preheating of the target material.

Original construction of Ranges S-1 and S-2 was performed at the Air Proving Ground Center, AFSC, Eglin Air Force Base, Florida. Since the transfer of the ranges to AEDC, part of the launcher system and instrumentation have been modified to improve performance.

2.0 LAUNCHER SYSTEMS FOR RANGES

The launcher systems (basically an NRL powder-driven, two-stage, light-gas gun design) for Ranges S-1 and S-2 are identical, allowing gun

---

Manuscript released by author April 1962.

components to be interchanged. The pump tubes are smooth bore, 37-mm, 64-caliber-long antitank guns. The high pressure section, which has an OD to ID ratio range of 4.5 to 6, allows final pump tube pressures of 300,000 psi or more. Launch tubes presently used are 30 calibers by 5 ft long. This length can be varied from 120 to 400 calibers by using a lined launch tube.

Energy input to the launcher is provided by a charge of small arms propellant, which is used to drive the plastic piston which, in turn, compresses a light gas (He or H_2) in front of it to a high pressure and temperature. This high energy gas then propels the projectile through the launch tube.

These launcher systems are capable of accelerating a 0.4-gram (total weight), saboted projectile to 26,000 fps.* Figure 3 shows the present S-1 and S-2 launch capabilities, weight of projectiles, and sabot vs maximum velocity.

A third launcher is being constructed to launch 0.5-in.-diam projectiles. The predicted performance, which is based on experience gained with S-1, S-2, and existing 0.5-in.-caliber launchers, indicates a capability of launching a one-gram projectile to 30,000 fps.

3.0 RANGES

The overall length of Ranges S-1 and S-2 is approximately 80 ft, although the projectile travels approximately 55 ft. Range S-1 is basically the same as S-2 (Fig. 2).

The current tests are being conducted with targets which are 12 by 12 in. and vary from 1 to 3.5 inches in thickness. The 12 by 12-in. target size has been chosen to ease alignment of the launcher and to save target material. In most cases four data shots can be made using one target. There is dispersion of ±1.5 in. from the aligned trajectory. Multiple thin plates would be limited to 6-in. total depth since the present optical recorder has a 7-in.-diam field of view at the center of the target.

The heaters (on Ranges S-2 and S-3), which are used to preheat the targets, are provided with 30 quartz-tungsten filament lamps. These heaters provide sufficient thermal energy to heat a metallic target to 1500°F.

---

*W. B. Stephenson. "Performance of a Small Two-Stage, Light-Gas Gun Used for Impact Testing." AEDC-TN-61-166, January 1962.

Range S-3, which is scheduled for completion in June 1962, has an expansion and target chamber of 6 ft in diameter by 21 ft long. The target chamber has been installed and operated to 10^{-6} mm Hg. The target can be prestressed to 100,000-lb tension in two directions, preheated to a temperature of 1500°F, and positioned to the trajectory at any angle between 0 and 90 deg. These events can be performed while maintaining a given vacuum level throughout the range. Comparison of pertinent data concerning the three Terminal Ballistics Ranges is shown in Table 1.

4.0 INSTRUMENTATION FOR RANGES

Figure 4 shows a block diagram of the present range instrumentation and firing control circuits. The shadowgraphs use a spark discharge for a light source and can be used with or without a Kerr cell. The spark duration is 0.25 microsecond, but exposure time can be limited to 0.06 microsecond with the use of the Kerr cell. The Berkeley counters (Model 7370, 10-megacycle) are activated by a trigger when the projectile is in the shadowgraph's field of view. Thus, an accurate time and distance between shadowgraph stations is known. The primary velocity measurements are made with a Beckman & Whitley (B & W) Model 192 framing camera. This camera has a maximum framing rate of 1.4×10^6 frames/sec. The xenon tube, which illuminates the B & W camera's field of view, can be adjusted for light durations from 30 to 200 microseconds. This allows proper exposure of 82 frames without rewrite or the use of a blast shutter. Optical coverage from this camera is available on Ranges S-1 and S-2. Figures 5a and b show two series of photographs, which were obtained from the B & W negatives, of a plastic right circular cylinder (0.3 inch in diameter by 0.3 inch long) impacting into a transparent plastic target.

5.0 PHYSICS OF CRATER FORMATION

In current impact studies only post-event measurements of the crater are obtained, i. e., crater diameter, depth, and volume. Crater volume data for semi-infinite targets is shown in Fig. 6. Appendix I describes the measurement procedure. There are other parameters which may be measurable, and the feasibility of these measurements is discussed.

5.1 STRESS ANALYSIS OF CRATERS

Equipment for photoelastic studies of transparent models is available. A study will be necessary to determine if a compatible transparent model can be found. The other present technique for dynamic stress analysis is to apply a photoelastic coating to an oblique object and photograph the coating during the stressing event. If sufficient lighting can be obtained for the high-speed photography, the stress coating technique may be of value.

5.2 RADIATION MEASUREMENTS

Presently, there are no experimental data available pertaining to the energy dissipation during the crater formation. Part of the kinetic energy of the projectile is known to be dissipated as thermal radiation during the early phase of a crater formation. Measurement of energy distribution would help determine the basic physics of crater formation.

TABLE 1

DESCRIPTION OF TERMINAL BALLISTIC RANGES

Range	S-1	S-2	S-3
Target Chamber Diameter	3'	3'	6'
Connecting Tube Diameter (ID)	6"	6"	8"
Expansion Tank Diam/Length/No.	3'/3.5'/2	6'/sphere/2	6'/21'/1
Total Length	80'	80'	100'
Projectile Tube Size	0.30 or 0.50 caliber	0.30 or 0.50 caliber	50 calibers
Driver Gas	He or H_2	He or H_2	He or H_2
Max. Velocity/Projectile	26,000 fps/ 1/16 Al sphere 23,500 fps/ 1/8 Cu sphere	26,000 fps/ 1/16 Al sphere 23,500 fps/ 1/8 Cu sphere	30,000 fps/ 1/8 Cu sphere (est.)
First Stage	Solid propellant	Solid propellant	Solid propellant & H_2
Minimum Range Pressure	1 mm Hg	1 mm Hg	10^{-6} mm Hg
Target Specimen Preheat Capability	None	1500°F	1500°F
Preload Capability	None	None	100,000 lb in two directions
Velocity Measurements	Shadowgraph - 3 stations & B&W	Shadowgraph - 3 stations & B&W	Shadowgraph - 3 stations & B&W
B&W Field of View	7" diameter	7" diameter	8" diameter
Shadowgraph Field of View	3" diameter	4.5" diameter	4.5" diameter

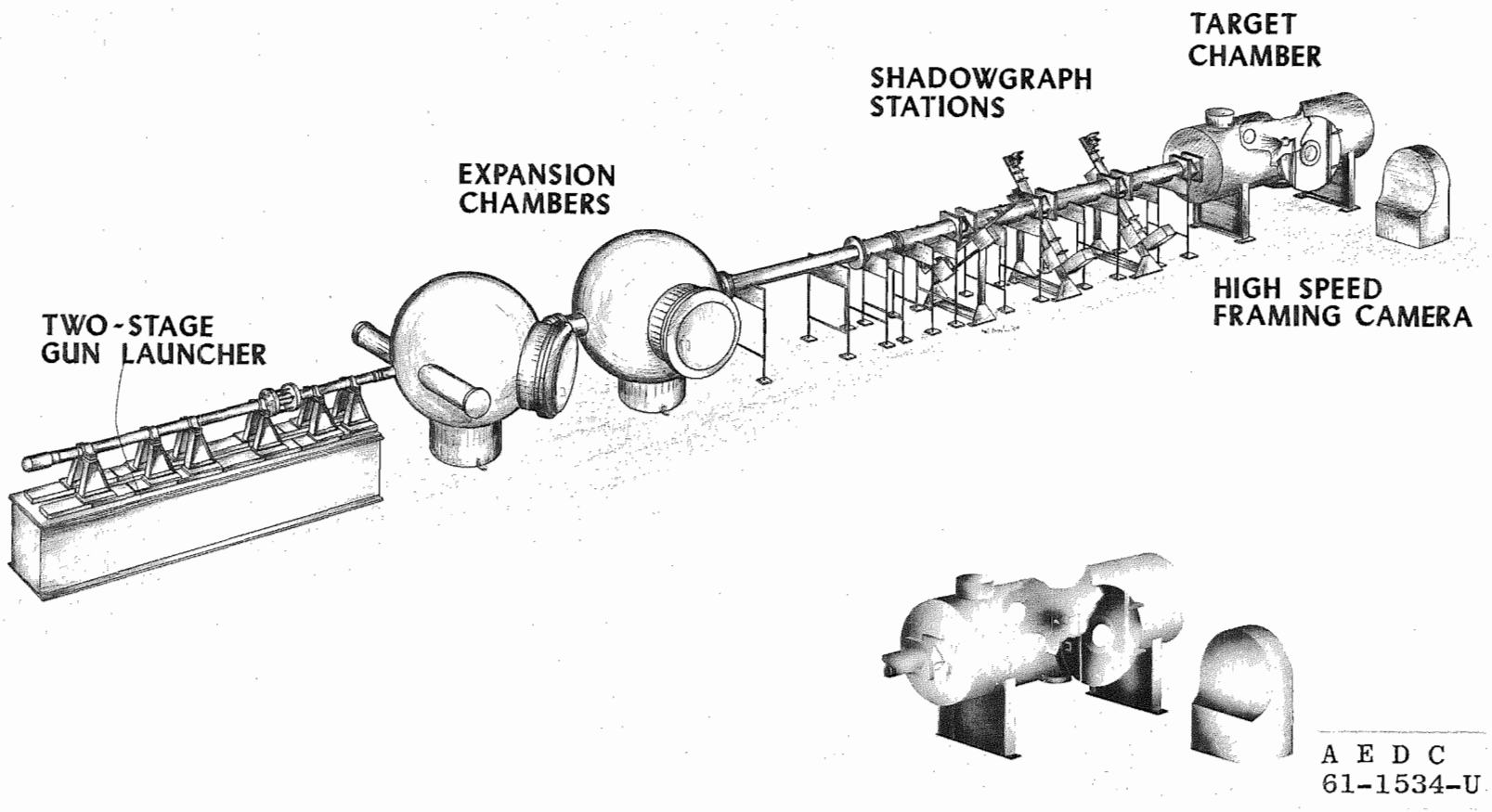

Fig. 1 S-2 Terminal Ballistics Range

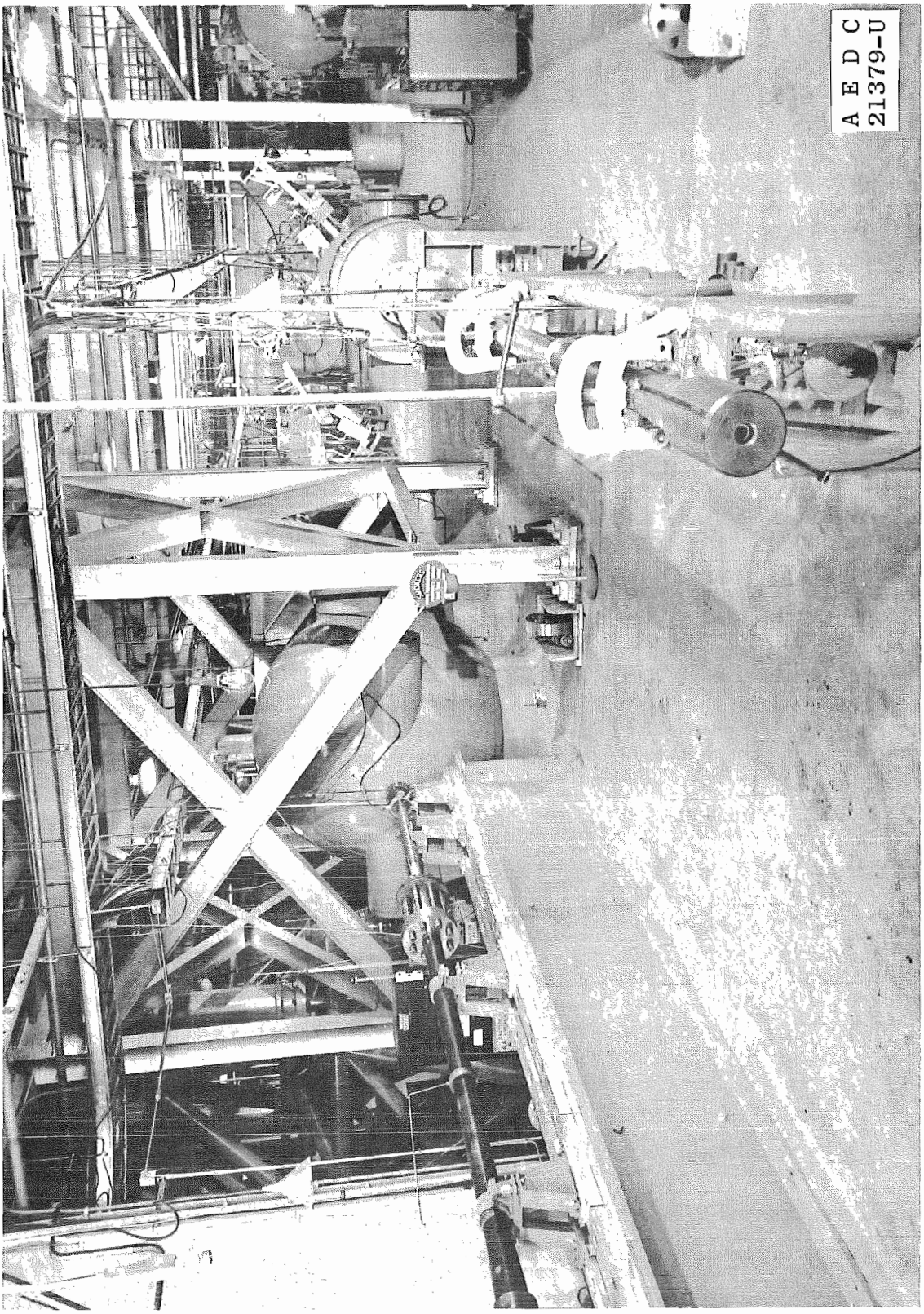

Fig. 2 S-1 and S-2 Terminal Ballistics Ranges

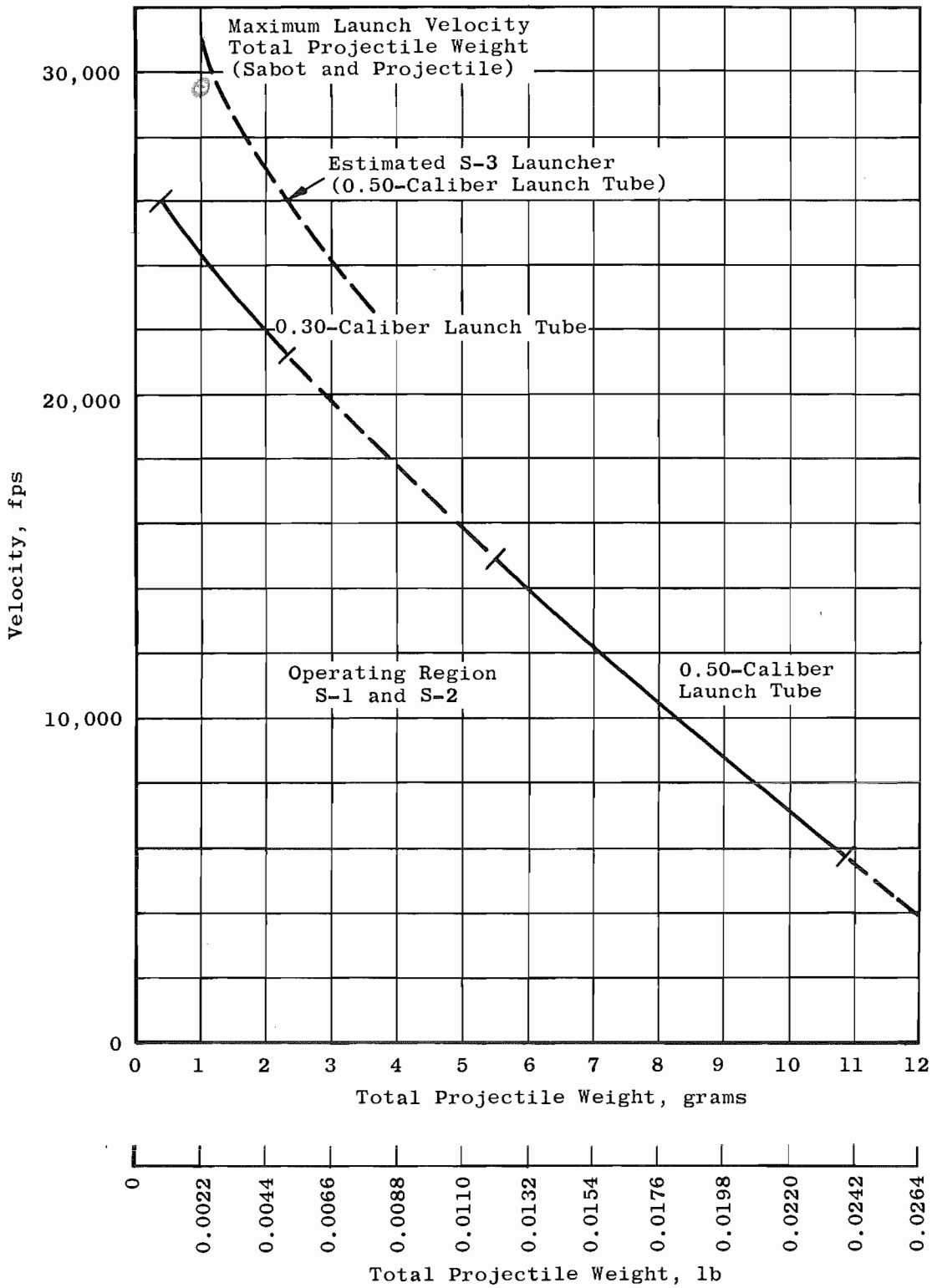

Fig. 3 Performance of S-1 and S-2

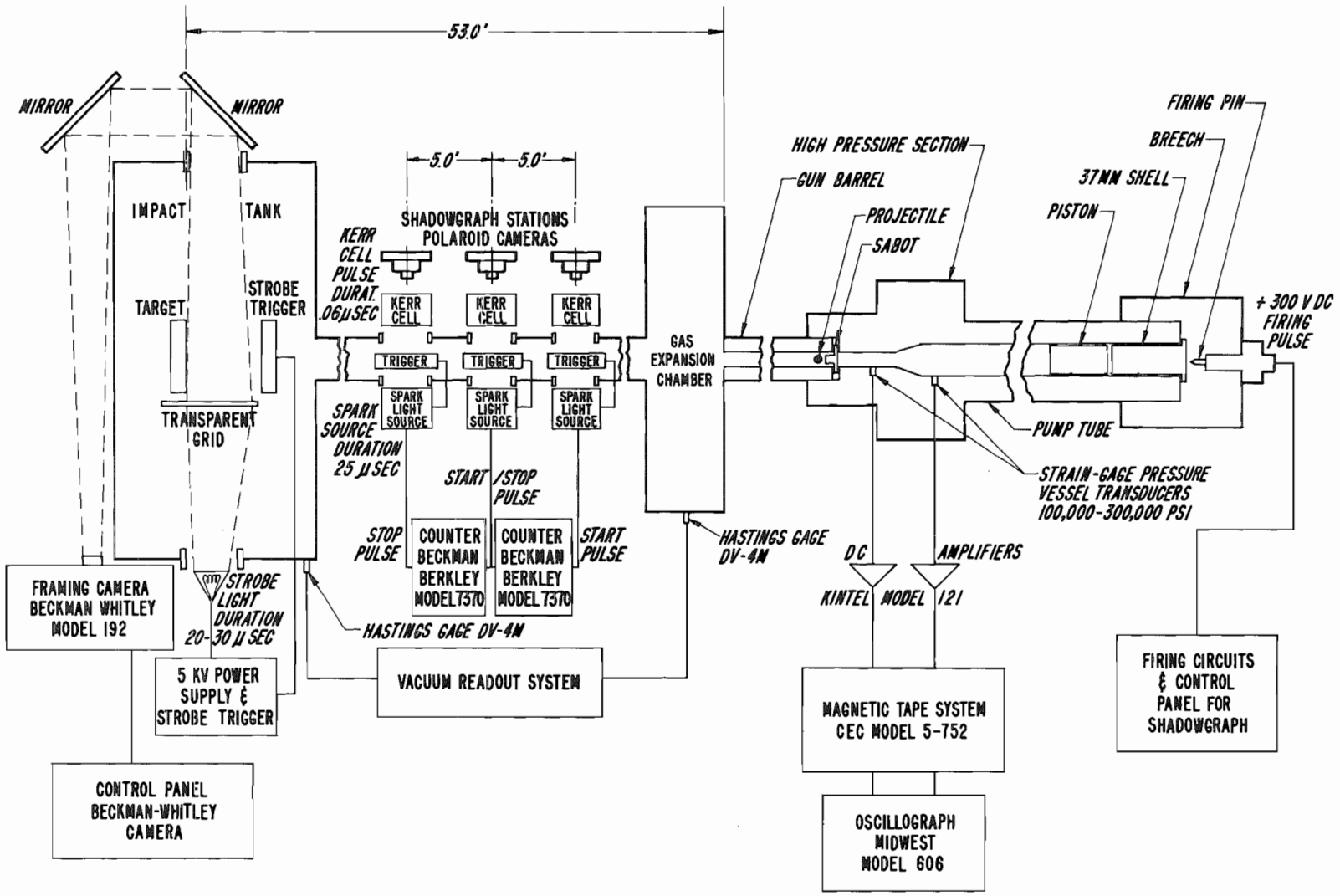

Fig. 4 Instrumentation for S-1 and S-2

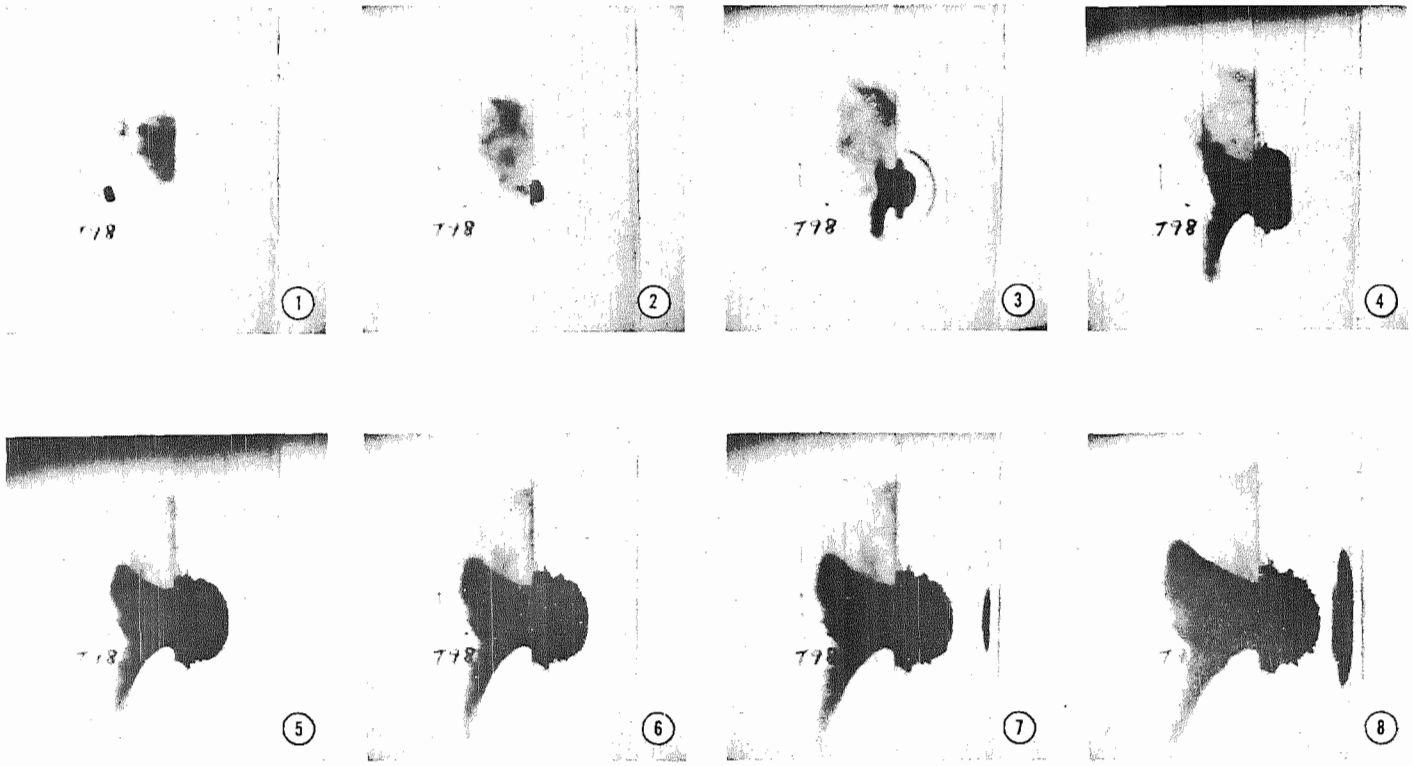

OBSERVATION OF HYPERVELOCITY IMPACT PHENOMENA

A test technique which enables the detailed observation of impact phenomena of a hypervelocity projectile has been developed in the von Kármán Gas Dynamics Facility. The above pictures show various stages of the projectile and back spall craters as follows: (1) plastic projectile approaching plexiglass target at 17,600 fps, (2) impact of projectile, (3, 4, and 5) development of projectile's crater and transit of shock wave through the target, (6) reflection of shock wave and formation of back spall crater, and (7 and 8) latter stages of crater formations.

a. 17,600 fps

Fig. 5 Observation of Hypervelocity Impact Phenomena

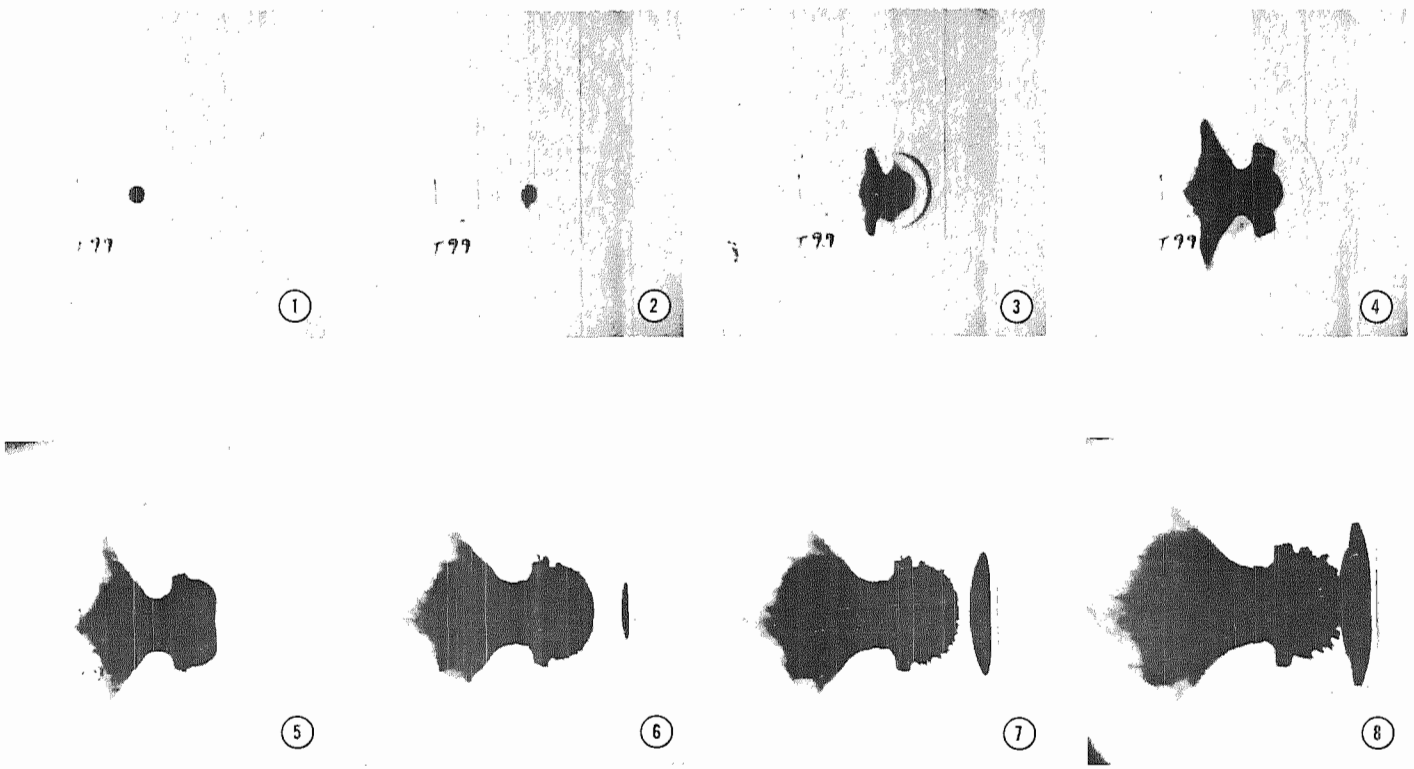

OBSERVATION OF HYPERVELOCITY IMPACT PHENOMENA

A test technique which enables the detailed observation of impact phenomena of a hypervelocity projectile has been developed in the von Kármán Gas Dynamics Facility. The above pictures show various stages of the projectile and back spall craters as follows: (1) plastic projectile approaching plexiglass target at 21,800 fps, (2) impact of projectile, (3, 4, and 5) development of projectile's crater and transit of shock wave through the target, (6) reflection of shock wave and formation of back spall crater, and (7 and 8) latter stages of crater formations.

b. 21,800 fps

Fig. 5 Concluded

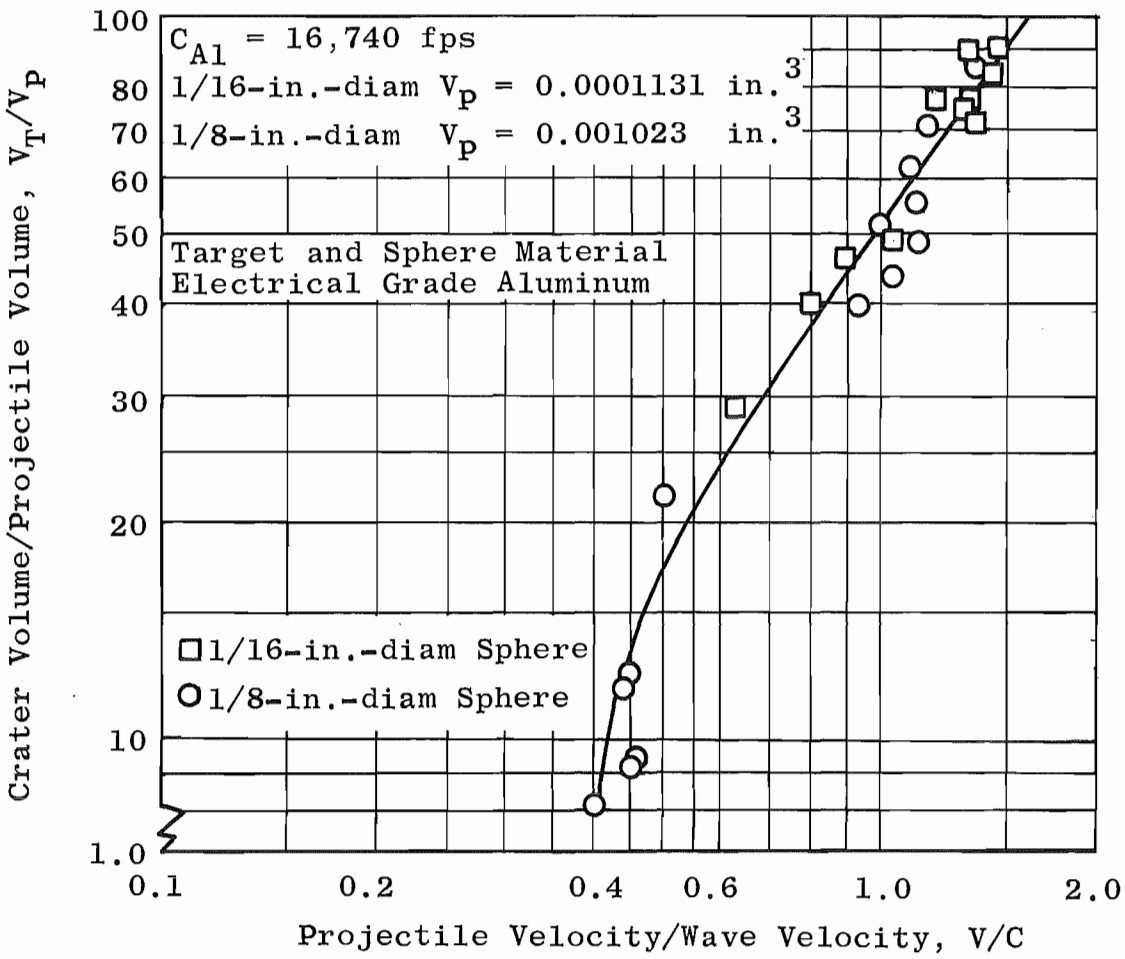

a. Volume

Fig. 6 Dimensions of Aluminum Impact Craters in Semi-Infinite Aluminum Targets

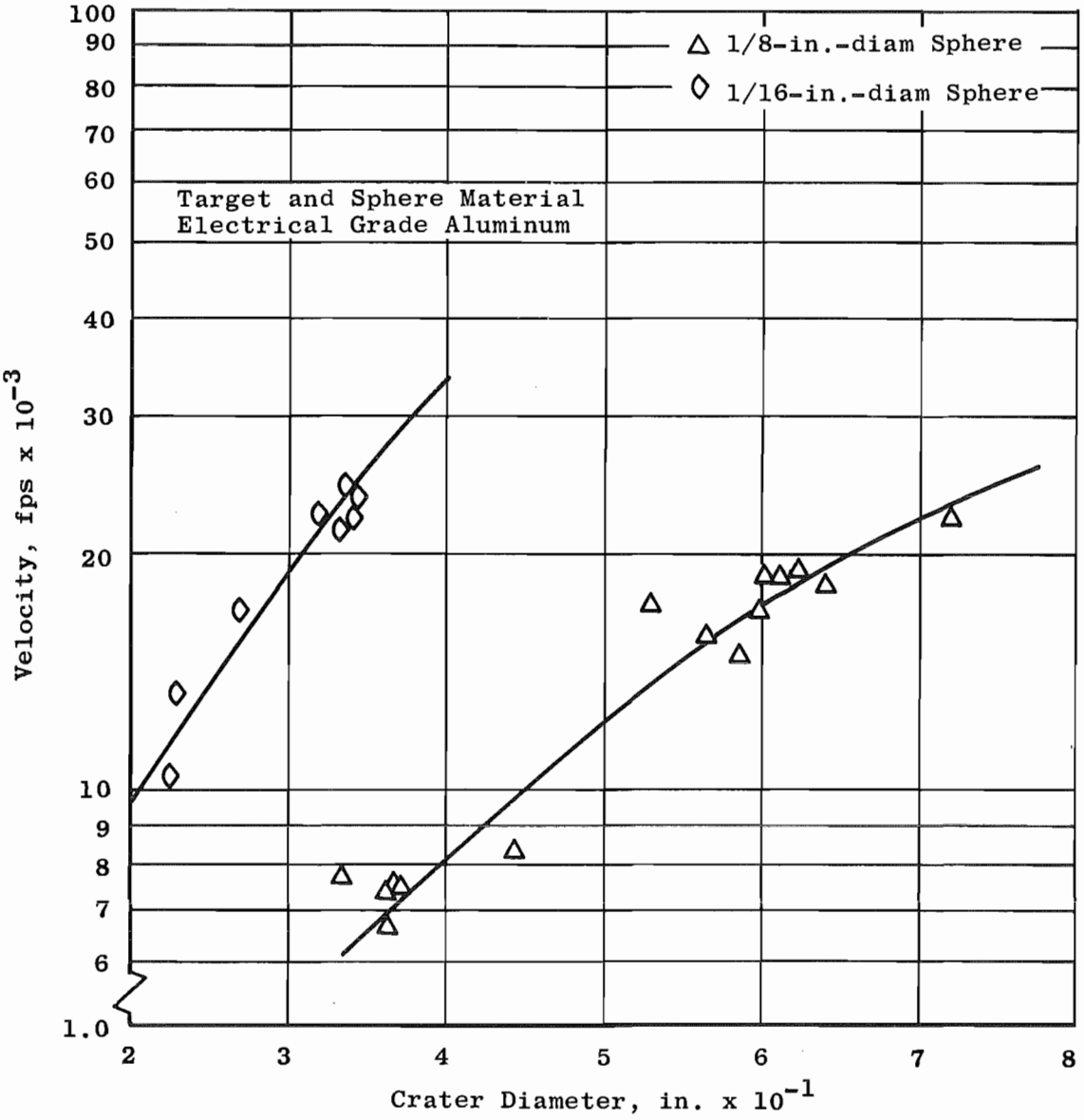

b. Diameter

Fig. 6 Continued

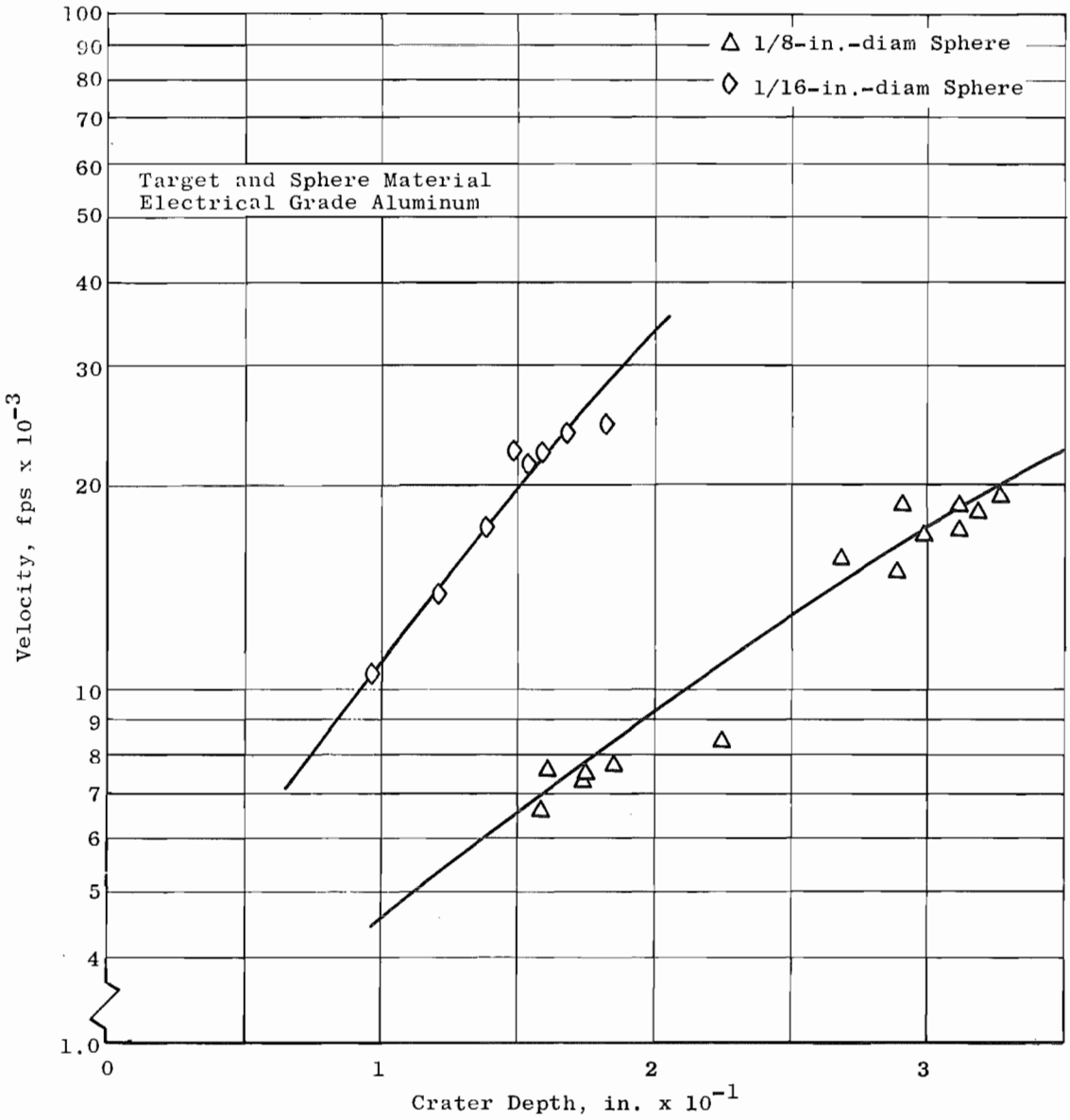

c. Depth

Fig. 6 Concluded

APPENDIX I

DATA REDUCTION

CRATER DIMENSION DETERMINATION

Measuring Equipment

A photograph of the equipment used for this experiment is presented in Fig. I-1. The unit consists of a 10-cc syringe, hypodermic needle, plexiglass syringe holder, telescope cathetometer, optical comparator table, liquid level indicator, optical and standard depth micrometer.

The plexiglass syringe holder is used to house the syringe and as an attachment for the depth micrometer. This unit's function is the metering of the liquid used in determining the volume and depth of the crater.

The cathetometer was used in conjunction with the optical comparator table and the liquid level indicator to obtain measurements of crater diameter and determination of liquid level.

Crater Dimensions

The crater volume is determined by filling the hole up to the original face plane of the target with an accurately metered amount of liquid.

A wetting agent (Alchonox) was used to eliminate the error caused by meniscus. Figures I-2a, b, c, and d show the contact angle between aluminum and tap water, distilled water, alcohol-water, and Alchonox-water solutions. Removal of impurities from the solution and foreign material from the crater surface is essential to minimizing the contact angle; these impurities may be eliminated from metal targets by sonic cleaning.

In determining crater volume, the area of the syringe piston is determined by measurements along the piston barrel. Next, the syringe is filled with solution and inserted in the fixture, and the depth micrometer is attached; then, by recording the distance through which the depth micrometer moves, the crater volume (volume = area x displacement) can be calculated. A graph showing metered volume as a function of piston displacement is shown in Fig. I-3.

To determine when sufficient solution has been added, a sheet metal liquid level indicator is used, as shown in the figure on the following page:

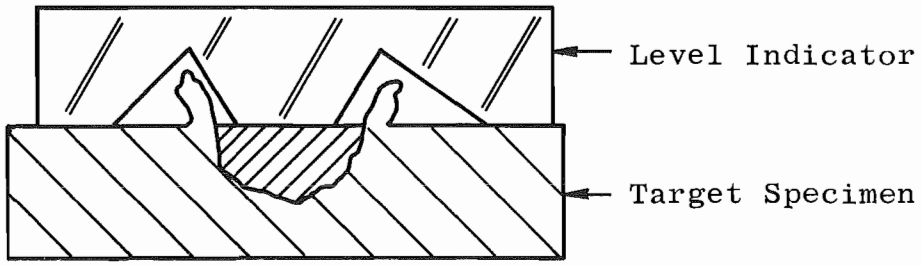

The solution metered into the crater is observed by the cathetometer telescope, thus allowing the monitoring of the contact between the indicator and the liquid.

The crater diameter is measured by using the cathetometer and the vernier table of an optical comparator. The table of the optical comparator will be traversed until the cross-hairs of the cathetometer telescope are tangent to the opposite side of the crater at solution contact level. Therefore, the distance through which the optical comparator table traveled is equal to the diameter of the crater at that solution level. The depth of the craters produced in the target is determined by the use of an optical depth micrometer.

The evaporation rate of the one-percent Alchonox-water solution is one percent per hour as determined from a 0.36-in.^{2} surface area at 78°F and 28.98 in. of mercury. Since all of the measurements (on one crater) are made within five minutes, the error attributed to evaporation is considered to be negligible.

Accuracy of Measurements

To determine the accuracy and repeatability of the volume measuring technique, two hemispherical craters were machined in a metal target. The calculated volume of the craters was compared with the volume derived by using the metered Alchonox-water solution. The difference was less than one percent.

The volume measuring technique was also checked by weighing the amount of fluid that was metered into a crater. The results of this test are shown in Fig. I-3. The maximum difference between these two methods is less than one percent. Volumes measured by the fluid metering apparatus are repeatable to ±0.3 percent.

The depth as determined by the optical depth micrometer is repeatable to within ±0.0002 in.

Readings are taken at 90-deg intervals, and an average of these readings is the reported crater diameter. The diameter measurement (for a given position) is repeatable to ±0.001 in. for three measurements.

PROJECTILE VELOCITY DETERMINATION

The high-speed camera (B &W) has an electronic counter measuring turbine speed from which the framing rate may be derived. Therefore, with the time between frames and a measured distance that the projectile has moved between frames, one may derive projectile velocity. Since the distance parameter is relatively small, at least 20 frames are read along the trajectory. With the use of a computer, these data points are fitted with a Gaussian least squares fit to a linear curve. Maximum standard error is specified at 0.6 percent. If there is a larger deviation than 0.6 percent, the film is read again using all the frames available. The maximum error in the electronic counter from which time between frames is derived is one part in 500 or 0.2 percent. Thus, the maximum error is less than one percent.

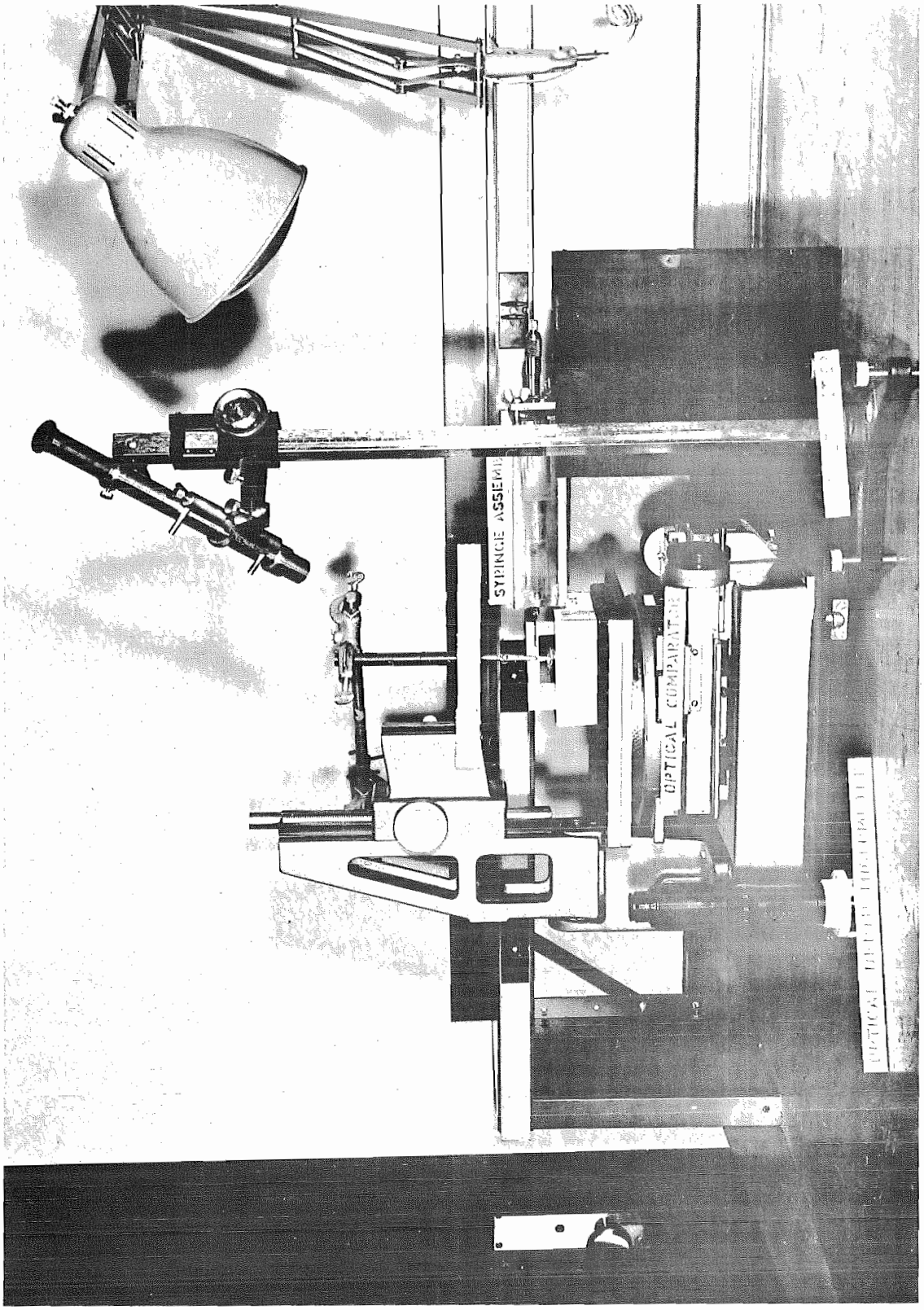

Fig. I-1 Apparatus Setup Used for Crater Dimension Determination

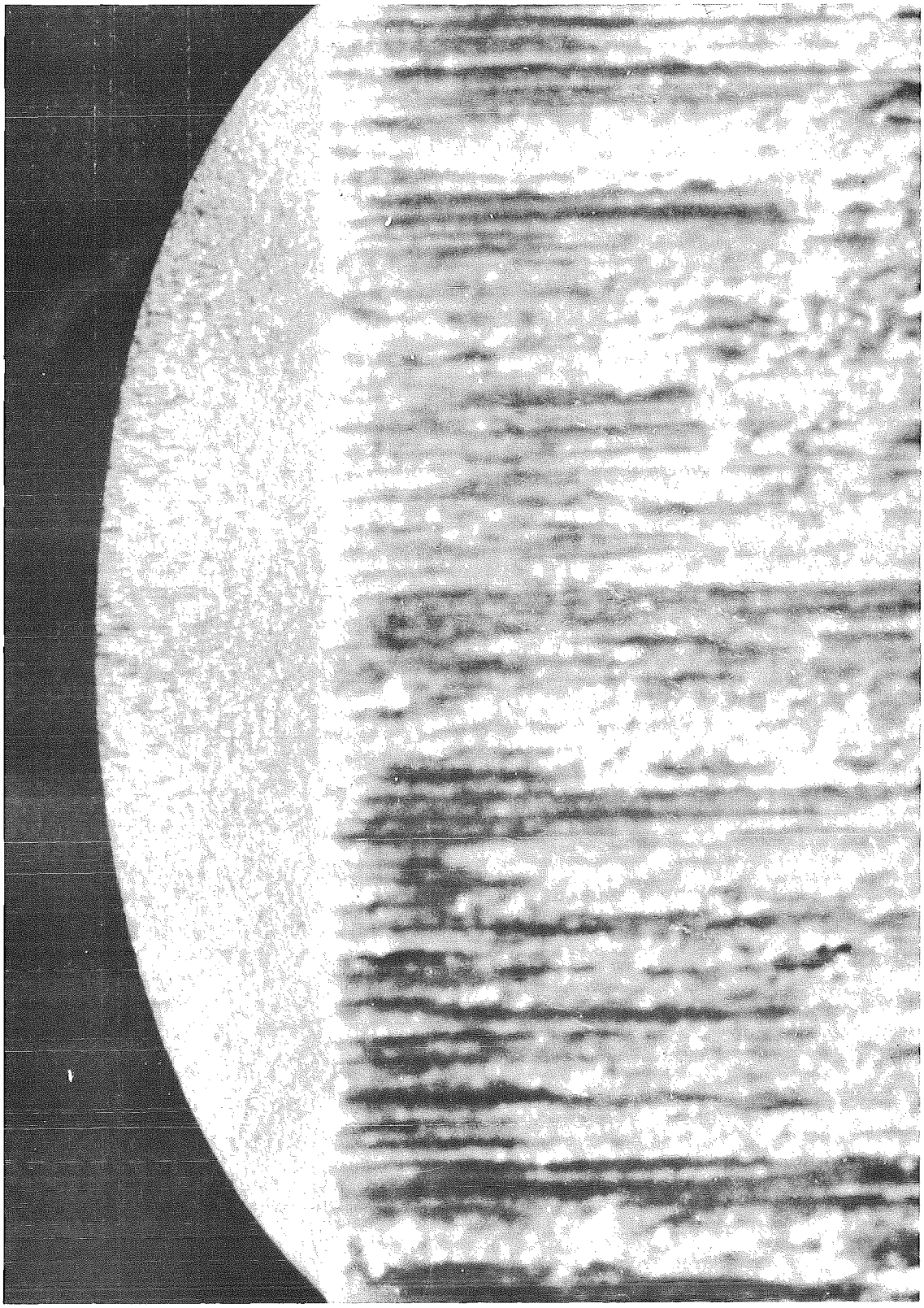

Fig. 1-2a 2-S Aluminum – Tap Water – Air/Contact Angle = 42° 50′

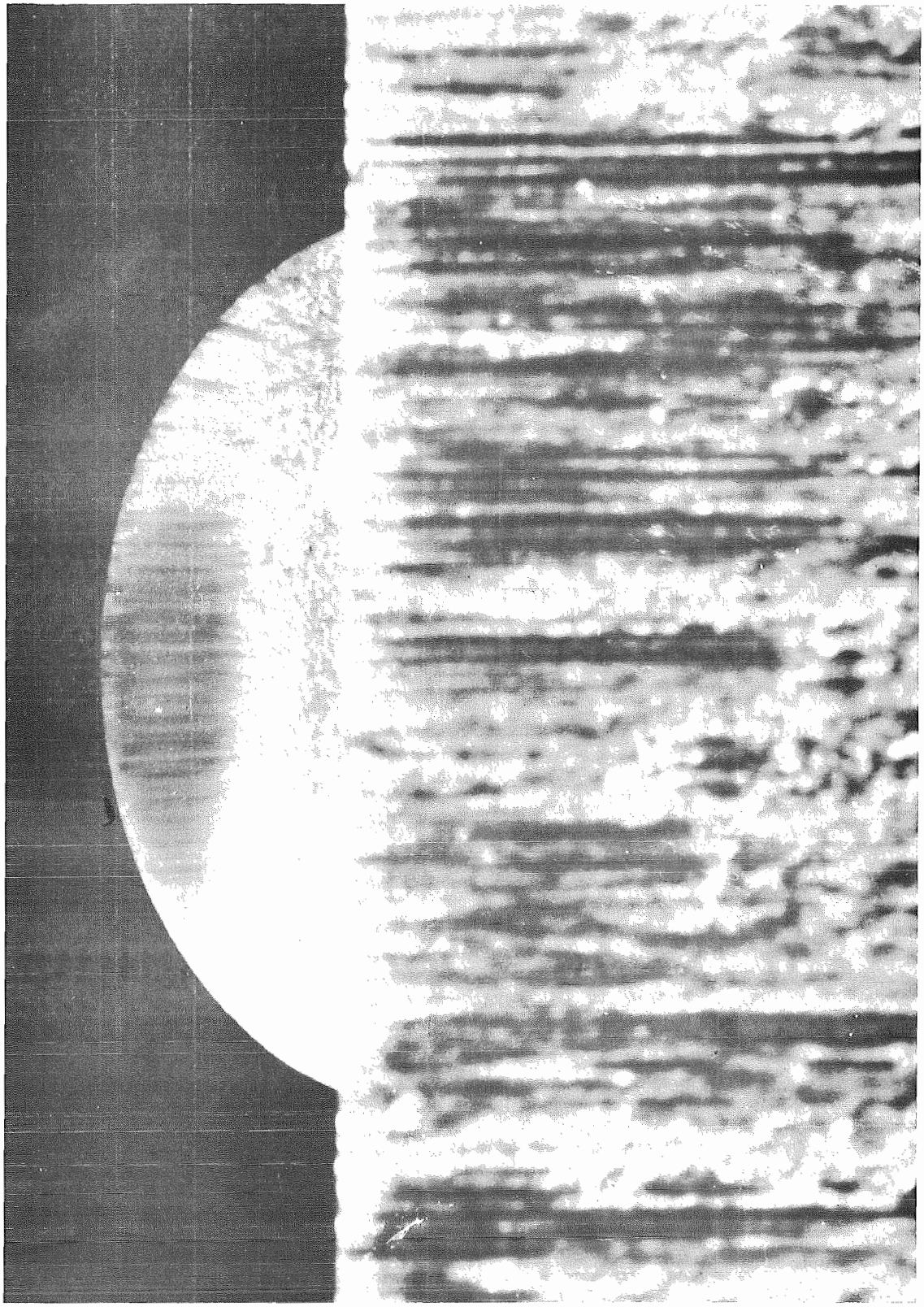

Fig. 1-2b 2-S Aluminum – Distilled Water – Air/Contact Angle = 64° 40′

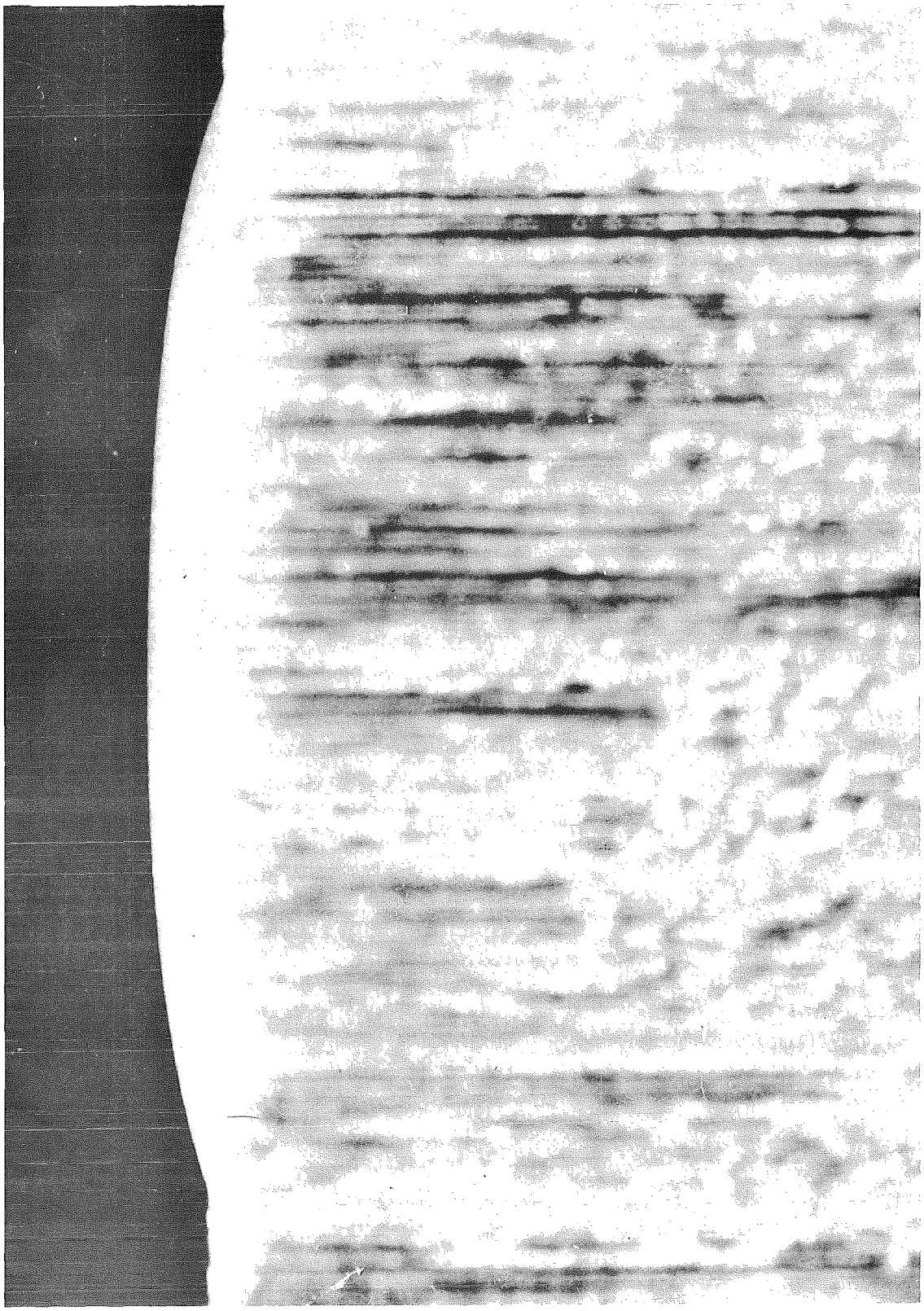

Fig. I-2c 2-S Aluminum – 50% E_tOH – Air/Contact Angle ≈ 22° 16′

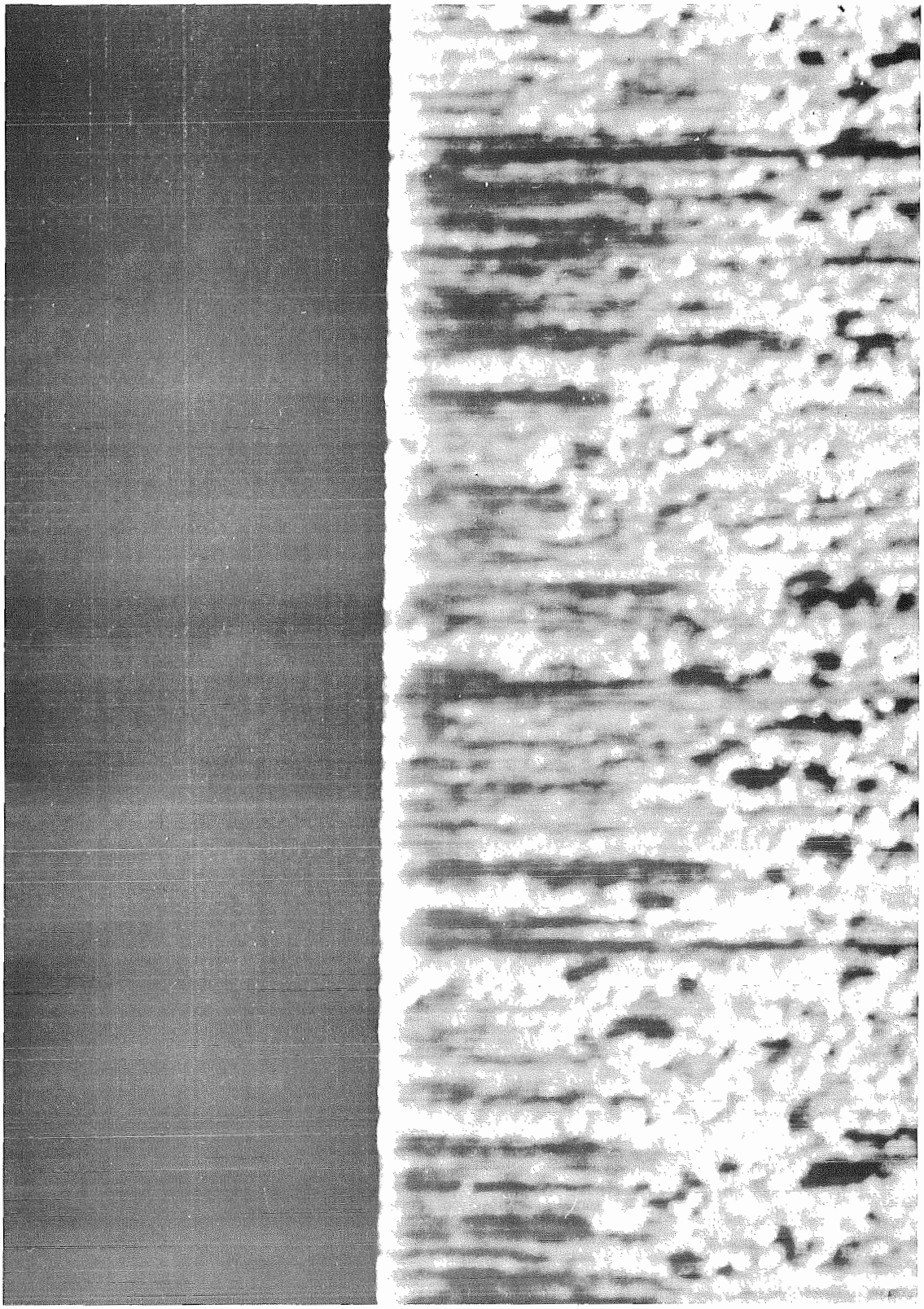

Fig. I-2d 2-S Aluminum – 1% Alchonox

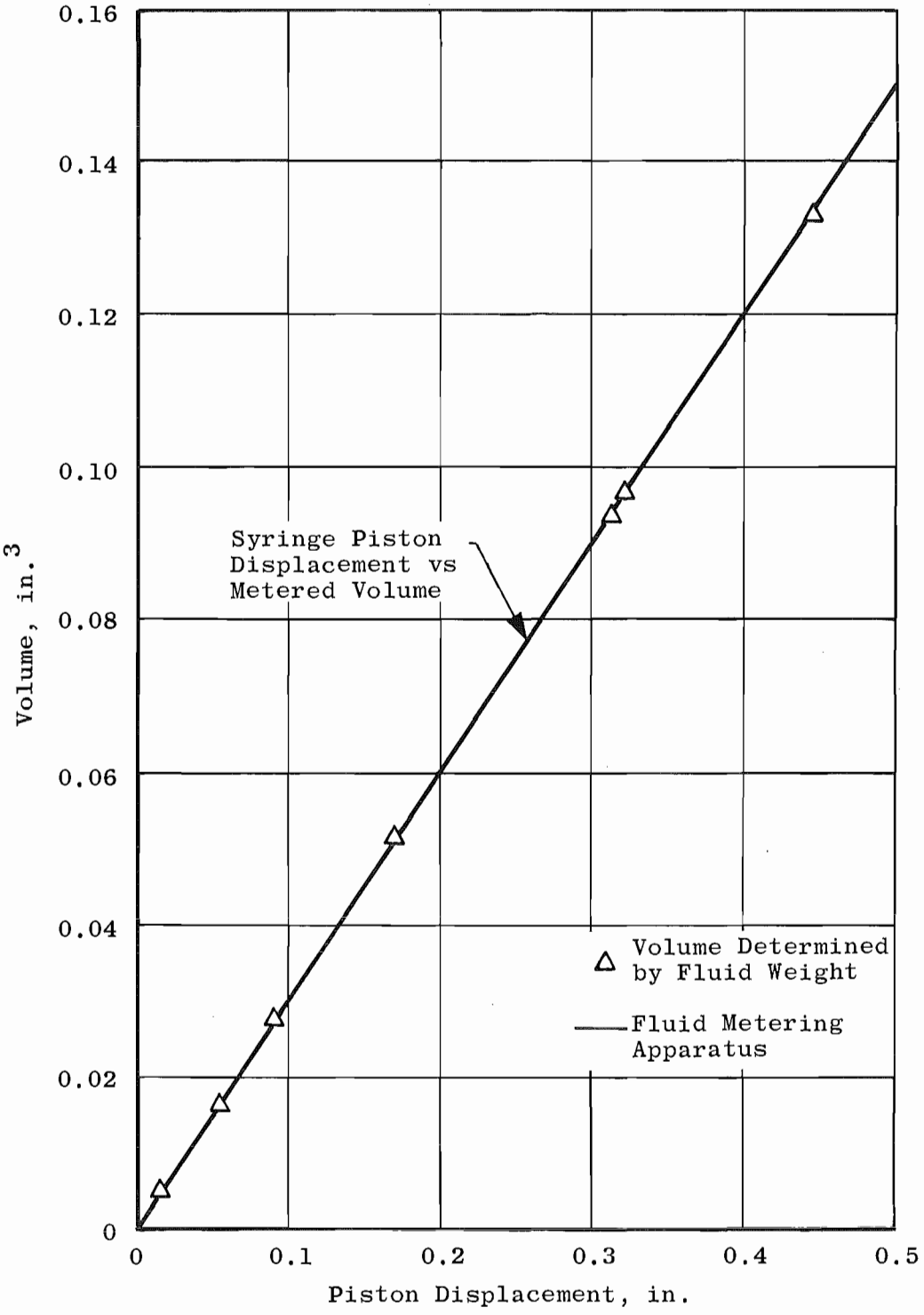

Fig. I-3 Calibration of Fluid Metering Apparatus